ACS APPLIED BIO MATERIALS

www.acsabm.org Article

Fabrication of Tunable 3D Cellular Structures in High Volume Using Magnetic Levitation Guided Assembly

Rabia Onbas and Ahu Arslan Yildiz*

Cite This: *ACS Appl. Bio Mater.* 2021, 4, 1794–1802 Read Online

ACCESS | Metrics & More | Article Recommendations | Supporting Information

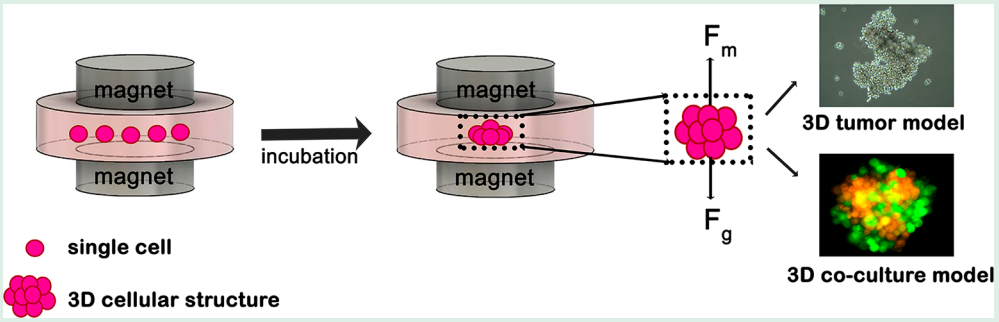

ABSTRACT: Tunable and reproducible size with high circularity is an important limitation to obtain three-dimensional (3D) cellular structures and spheroids in scaffold free tissue engineering approaches. Here, we present a facile methodology based on magnetic levitation (MagLev) to fabricate 3D cellular structures rapidly and easily in high-volume and low magnetic field. In this study, 3D cellular structures were fabricated using magnetic levitation directed assembly where cells are suspended and self-assembled by contactless magnetic manipulation in the presence of a paramagnetic agent. The effect of cell seeding density, culture time, and paramagnetic agent concentration on the formation of 3D cellular structures was evaluated for NIH/3T3 mouse fibroblast cells. In addition, magnetic levitation guided cellular assembly and 3D tumor spheroid formation was examined for five different cancer cell lines: MCF7 (human epithelial breast adenocarcinoma), MDA-MB-231 (human epithelial breast adenocarcinoma), SH-SY5Y (human bone-marrow neuroblastoma), PC-12 (rat adrenal gland pheochromocytoma), and HeLa (human epithelial cervix adenocarcinoma). Moreover, formation of a 3D coculture model was successfully observed by using MDA-MB-231 dsRED and MDA-MB-231 GFP cells. Taken together, these results indicate that the developed MagLev setup provides an easy and efficient way to fabricate 3D cellular structures and may be a feasible alternative to conventional methodologies for cellular/multicellular studies.

KEYWORDS: *magnetic levitation, scaffold-free tissue engineering, 3D cell culture, 3D tumor spheroid, contactless manipulation*

1. INTRODUCTION

Cell culture is an important tool for tissue engineering and regenerative medicine, drug screening and efficacy evaluation, and tumor and disease modeling studies.[1−5] Due to limitations of conventional two-dimensional (2D) cell culture in mimicking native tissues, recently three-dimensional (3D) cell culture models have started to be utilized.[6−12] 3D cell culture models are a promising approach for various applications[13−18] since they mimic the native tissue-specific physiological microenvironment very closely. Spheroids are known as significant 3D cellular models, especially for pharmaceutical and therapeutic studies, because *(i)* they represent diffusion-limited *in vivo* tissue models, *(ii)* they comprise oxygen and nutrient gradients that resulted in a necrotic core, *(iii)* the radially symmetric structure of spheroids allows formation of a diffusion gradient, and *(iv)* it enables coculturing multiple cells that can mimic heterogeneous tissue structure.[19−23] Spheroid structures have been fabricated through various methods such as hanging drop, nonadhesive surfaces, and spinner flask.[24−27] Nonadhesive surfaces and spinner flasks are very simple methods, and mass production is possible. However, tuning properties of spheroids, for example, controlling cell number, spheroid size, and shape, is not possible.[28,29] Hanging drop is one of the most common methods to fabricate spheroids, since it is a simple, easy-to-use, and cost-effective methodology.[30] Regardless of the ease of use, there are certain limitations of the hanging-drop technique; spheroid formation occurs in a low volume where the cell medium cannot be easily changed and results in restricted spheroid size, and due to low volume bulk production is laborious.[31]

Received: November 22, 2020
Accepted: January 11, 2021
Published: January 25, 2021

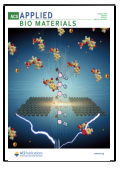

https://dx.doi.org/10.1021/acsabm.0c01523
ACS Appl. Bio Mater. 2021, 4, 1794–1802

Recently, a new tool, the "magnetic levitation technique", gained popularity, which was developed to form spheroids and 3D cellular structures.[8,32−35] Magnetic levitation works on the use of the magnetic field principle to accumulate cells at a certain levitation height. When cells are accumulated at the same levitation height, cell−cell interaction increases that leads to cellular aggregate and spheroid formation. Magnetic levitation technology allows contactless manipulation of cells and spatial control in 3D where cell−cell interaction is favored, and cells can create their own extracellular matrix (ECM) microenvironment, as well as formation of more complex and heterogeneous 3D cellular structures being promoted. This technique has been used to form both scaffold-based and scaffold-free 3D cellular models, as well as coculture, homogeneous, and heterogeneous 3D cellular assemblies, and tumor models have been formed.[8,32,36−41] Despite various successful applications as 3D cell culture model, there are few drawbacks of recently reported systems such as use of nanoparticles or scaffold materials, requirement of sophisticated and expensive setups or optical components, limited volume and scale-up difficulties. We recently used magnetic levitation methodology to fabricate 3D cellular structures.[8] Although it is simple and easy-to-use setup, the cell culture volume is limited to only 30 μL, change of cell medium is not possible, and optical components are needed for screening of cellular structures.

In order to overcome such obstacles, a new high-volume (800 μL) MagLev setup that allows formation of tunable 3D cellular structures and spheroids is proposed in this study. The methodology reported here provides certain advantages over standard 3D methodologies because it is simple, rapid, and cost-effective, it provides easy and contactless magnetic manipulation of cells in high-volume and low magnetic field, it is applicable to various cell lines and analysis methodologies, and formed 3D cellular structures can be easily visualized under a basic light microscope without any optical components. As a proof of concept, 3D cellular structures of NIH/3T3 with controlled size and circularity were formed. The size, area, and circularity of the spheroids were controlled by tuning cell seeding density, paramagnetic agent concentration, and cell culturing time. Basic characterization was done to demonstrate cell viability and ECM formation. Moreover, the capability of the methodology was validated for 3D tumor spheroid formation by magnetic levitation guided culturing of five different cancerous cell lines. Finally, to further investigate the ability of the MagLev system coculture formation was investigated by using MDA-MB-231 dsRED and MDA-MB-231 GFP cells. Overall, these findings show that this platform holds promise for scaffold-free tissue-engineering applications.

2. MATERIALS AND METHODS

2.1. Design and Development of High-Volume MagLev Setup for 3D Cell Culture. The developed MagLev setup is given in Figure S1. These setups consist of two permanent Neodmiyum (NdFeB) disc magnets, which are arranged in an anti-Helmholtz configuration and integrated in poly(methyl methacrylate) (PMMA) holders. To investigate the levitation behavior of cells and formation of 3D cellular structures, either 40 × 5 mm (0.15 T) or 30 × 15 mm (0.4 T) NdFeB N35 magnets (Mıknatıs Teknik Company) were used. The magnetic field strength of the magnets was measured as 0.15 T and 0.4 T for 40 × 5 mm and 30 × 15 mm magnets, respectively, by using GM07&GM08 Gmeter (Hirst Magnetic Instruments Ltd.). The fabricated MagLev setup was sterilized with UV and ethanol 70% prior to cell culture experiments. A Petri dish (Ibidi- 80131, 800 μL) that contains cells, complete cell medium, and paramagnetic agent Gx (Gadobutrol/Gadovist, Bayer) was placed inside the setup between the magnets for cell culture studies.

2.2. Standard Cell Culture. NIH/3T3 (mouse fibroblast, ATCC CRL-1658), MCF7 (human epithelial breast adenocarcinoma, ATCC HTB-22), MDA-MB-231 (human epithelial breast adenocarcinoma, ATCC HTB-26), SH-SY5Y (human bone-marrow neuroblastoma, ATCC CRL-2266), PC-12 (rat adrenal gland pheochromocytoma, ATCC CRL-1721), HeLa (human epithelial cervix adenocarcinoma, ATCC CCL-2), MDA-MB-231 dsRED, and MDA-MB-231 GFP cells were cultured in high glucose DMEM (GIBCO, Thermo Fischer Scientific) containing L-glutamine and supplemented with 10% Fetal Bovine Serum (GIBCO, Thermo Fischer Scientific) and 1% penicillin/streptomycin (GIBCO, Thermo Fischer Scientific). The cells were cultured up to ∼90% confluency in a humidified environment (5% CO_2, 37 °C). The harvested cells were used for further magnetic levitation studies.

2.3. Optimization of 3D Cell Culture Parameters via the NIH/3T3 Cell Line. First, cell number and spheroid size relation were investigated for varied cell numbers: 2.5/5/10/25/50/100 × 10^3 at 10 mM Gx (Gadobutrol) concentration, 0.15T magnetic field, and 24 h culturing time. Later, the levitation profiles of cells and toxicity of Gx were analyzed for 30/50/100 mM Gx at 0.15 T. Finally, to evaluate long-term cell viability and morphological changes of spheroids, they were incubated for 1/3/5/7 days at fixed Gx concentration, cell number, and magnetic field as 30 mM, 2.5 × 10^3 NIH/3T3, and 0.15 T, respectively.

Cell viability analysis of spheroids was carried out by Live/Dead assay. CytoCalcein Green and propidium iodide (PI) dyes (AAT Bioquest) were used in equal proportions and added into the assay buffer solution. Cells were stained with the dye solution at 37 °C for 30 min. Then, viability analysis was performed using a fluorescence microscope (Zeiss Axio Observer). Cell viability (%), spheroid area analysis, and circularity measurements were done by ImageJ software (NIH).

2.4. Characterization of 3D NIH/3T3 Self-Assembled Structures. To characterize and investigate the 3D cellular structures, nucleus, cytoskeleton, and collagen staining was done for short-term (1 day) and long-term (7 days) cultured spheroids. Spheroids were fixed with 4% paraformaldehyde for 20 min, permeabilized with 0.1% Triton X-100 in PBS for 5 min, and then blocked with 1% BSA in PBS for 30 min. For F-Actin labeling, TRITC-conjugated Phalloidin (Sigma-Aldrich) was applied for 60 min at room temperature (RT). After rinsing, anticollagen Type I-FITC (Sigma-Aldrich) was applied for 50 min at RT for labeling collagen I of extracellular matrix. DAPI (Sigma-Aldrich) solution was applied for 5 min prior to rinsing. After nucleus staining, rinsing was performed three times, and stained 3D structures were visualized under a fluorescence microscope (Zeiss Observer Z1).

2.5. Formation of 3D Tumor and 3D Coculture Model. To obtain 3D tumor models, varied cancer cell lines were used such as MCF7, MDA-MB-231, SH-SY5Y, PC-12, and HeLa. Cell density was kept as 10 × 10^3, and 10 mM of Gx concentration was applied for both. However, differently from MCF7, SH-SY5Y, and PC-12 cell lines, magnetic field was increased from 0.15 T (40 × 5 mm magnet) to 0.4 T (30 × 15 mm magnet) for MDA-MB-231 and HeLa cell lines to decrease the incubation time and obtain 3D cellular structures. Also, MDA-MB-231 dsRED and MDA-MB-231 GFP cell lines were performed to form a 3D coculture model. Total cell density and magnetic field were kept as 10 × 10^3 and 0.4 T, respectively, while Gx concentration was applied as 50 and 100 mM.

3. RESULTS AND DISCUSSION

3.1. Fabricating 3D Cellular Structures via Developed MagLev Setup. The developed MagLev setup is given in Figure S1. This platform is designed for easy and rapid formation of spheroids in high volume under low magnetic field by using the magnetic levitation methodology. In this technique, a cell culture solution containing a paramagnetic

https://dx.doi.org/10.1021/acsabm.0c01523
ACS Appl. Bio Mater. 2021, 4, 1794−1802

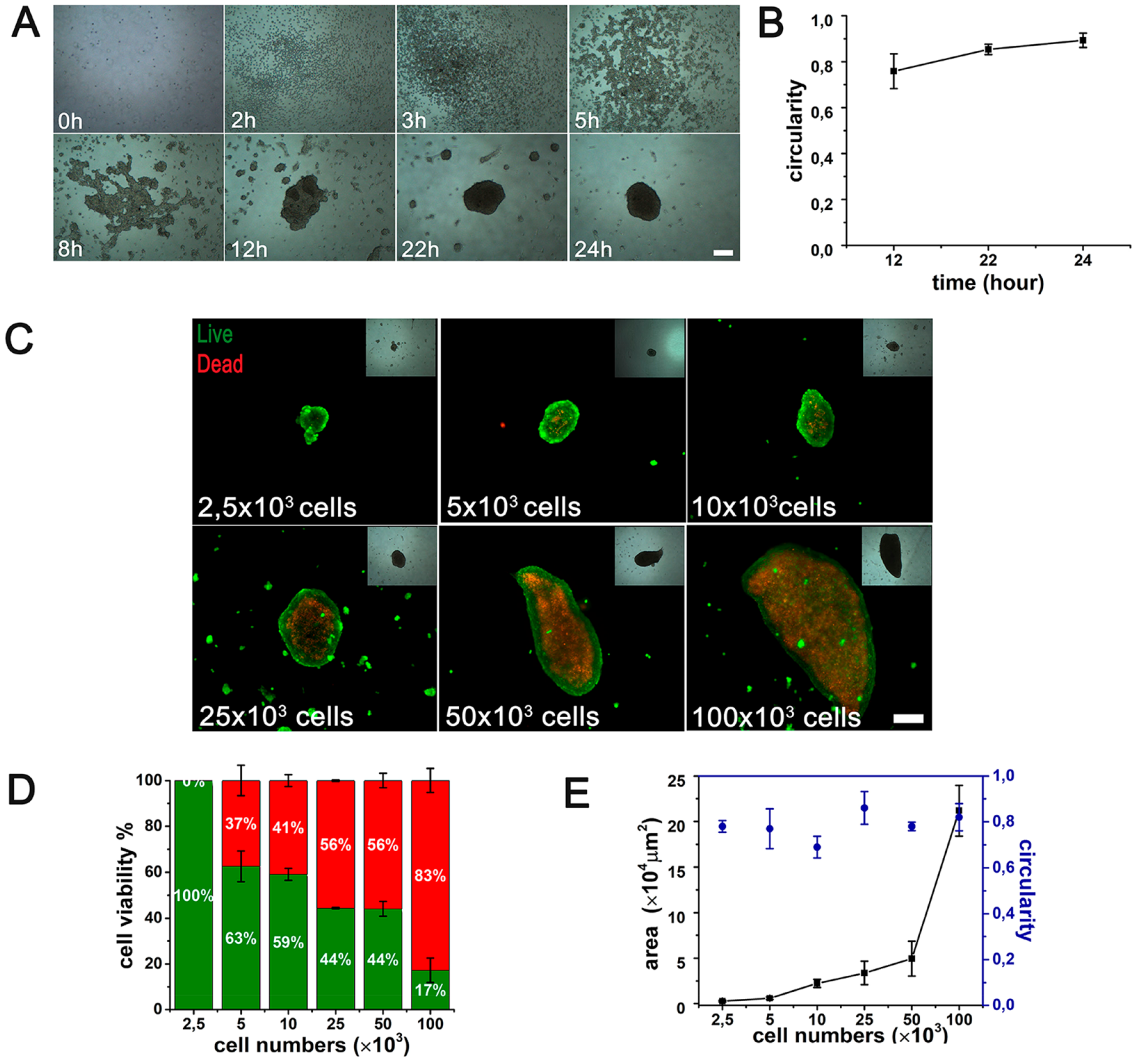

Figure 1. (A) Time-dependent light microscopy images of spheroid formation for NIH/3T3 cells via magnetic levitational assembly at various culture times (0, 2, 3, 5, 8, 12, 22, and 24 h). Scale bar: 200 μm. (B) Circularity values obtained from ImageJ for 25 × 10^3 cells at various culture times (12, 22, and 24 h). (C) Cell viability images of NIH/3T3 spheroids for various cell seeding densities (2.5, 5, 10, 25, 50, and 100 × 10^3) (green, live cells; red, dead cells) Scale bar: 200 μm. (D) Cell viability values of NIH/3T3 spheroids for various cell seeding densities (2.5, 5, 10, 25, 50, and 100 × 10^3). (E) Representative spheroid area versus circularity for various cell seeding densities (2.5, 5, 10, 25, 50, and 100 × 10^3).

agent (Gx) is placed between two magnets, which are assembled in the anti-Helmholtz configuration as shown in Figure S1B and S1C. In the magnetic levitation technique, cells are magnetically guided toward a lower magnetic field area from a higher magnetic field area in a paramagnetic medium. Colloidal cellular clusters start to form at the center of the Petri dish, where buoyancy forces are equalized by magnetic and gravitational forces.[8,36] Magnetically guided and accumulated cells form 3D cellular structures and spheroids due to increased cell−cell interactions at a certain levitation height. This newly designed configuration provides a way to tune the size and cellular properties of 3D cellular structures. Considering the MagLev setup that we have used in our previous work,[8] the newly developed setup; *(i)* enables easy and rapid fabrication of tunable 3D cellular structures in high volume and low magnetic field, *(ii)* offers significant profit for easy imaging and analysis of spheroids in real-time, and *(iii)* allows large scale production; moreover, *(iv)* its simplicity, low-cost, and portability make it a convenient platform for use in resource limited settings.

First of all, the formation of a 3D cellular structure via magnetic levitation was screened and observed for NIH/3T3 cells against culturing time in Figure 1A. Cellular assembly in 3D and spheroid formation was screened in real-time at varied culturing times: 0, 2, 3, 5, 8, 12, 22, and 24 h by light microscopy. Light microscopy images were directly taken from the top of the Petri dish where only side-views were screened by the previously used setup.[8] At 0 h, cells were suspended by magnetic forces at the liquid−air interphase, and at 2 h, cells started to gather at the center. Cellular aggregation was formed at around 5 h, and at around 8 h cellular aggregates were combined to form larger 3D structures. At around 12 h of culturing time, loose cellular aggregates became denser and started to form spheroid structures, where perfectly circular structures were observed after 24 h of culturing. Circularity is another important characteristic for 3D cellular structures, which represents the ideal circular structure of a spheroid when the value is close to 1.[42] Circularity is described as

$$\text{Circularity} = 4\pi(\text{area}/\text{perimeter}^2)$$

https://dx.doi.org/10.1021/acsabm.0c01523
ACS Appl. Bio Mater. 2021, 4, 1794−1802

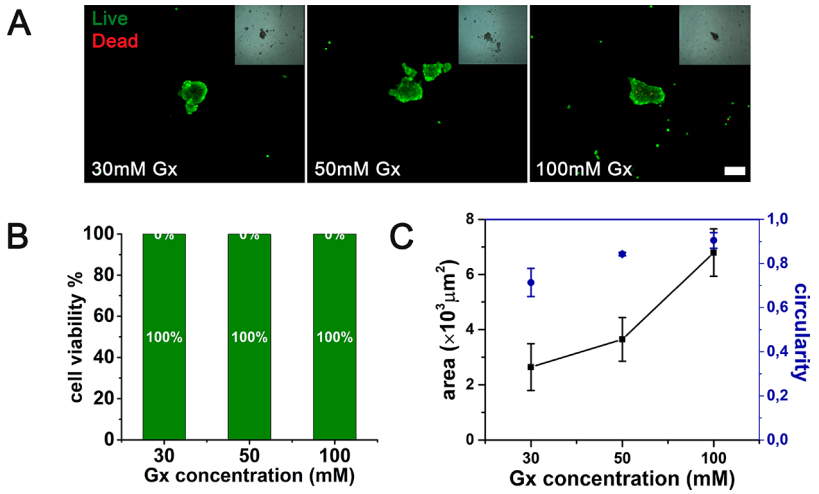

Figure 2. (A) Cell viability images of NIH/3T3 spheroids for various concentrations of Gx (30, 50, and 100 mM) for 2.5 × 10^3 cell seeding density. Scale bar: 200 μm. (B) Cell viability values of NIH/3T3 spheroids for various concentrations of Gx (30, 50, and 100 mM) for fixed 2.5 × 10^3 cell seeding density. (C) Representative spheroid area versus circularity for various concentrations of Gx (30, 50, and 100 mM).

As given in Figure 1B, the circularity of spheroids was calculated as 0.76, 0.85, and 0.89 for 12, 22, and 24 h culturing times, respectively.

3.2. Effect of Cell Seeding Density on Tunable 3D Cellular Structures. The size of a spheroid is an important parameter that affects the applicability of the spheroid in varied studies, such as drug screening. To investigate and then evaluate the effect of cell seeding density on spheroid size/area, a number of cells (2.5, 5, 10, 25, 50, 100 × 10^3) were cultured in 3D at 10 mM Gx. As shown in Figure 1C and 1D, a low density of cells (2.5, 5, 10 × 10^3) provided high cell viability that is ranging between 50 and 100%, while the viability decreased below 50% with the high density of cells (25, 50, 100 × 10^3). The reason for low cell viability was the diffusion limitation that occurs above 200 μm size of spheroids that prevent diffusion of O_2 and nutrients inside the spheroid, and also insufficient mass transport results in the accumulation of metabolic waste.[28,43] Spheroid area change was subsequently analyzed for varied cell numbers, where small spheroids were obtained with low cell density and bigger spheroids were obtained with high cell density (Figure 1E). Increased area of spheroids was observed as 0.26, 0.59, 2.22, 3.38, 4.94, and 21.2 × 10^4 μm^2, for varied cell numbers given as 2.5, 5, 10, 25, 50, and 100 × 10^3, respectively. Results confirm that spheroid size/area can be tuned by adjusting cell number. It is a well-known fact that large spheroids have diffusional gradient zones: (i) the outer layer consists of viable cells, and they can proliferate due to the well-oxygenated zone; (ii) the inner layer, known as the necrotic core, has hypoxic quiescent cells that cannot receive enough O_2, metabolites, and waste accumulation occurs in the core.[44,45] These layers were observed in large spheroids that were obtained from a high density of cells (Figure 1C). It was obvious that decreased cell number overcame diffusion limitations and resulted in high cell viability.

Also, Figure 1E represents circularity for varied cell densities. Circularity of spheroids in varied cell densities was changing between 0.69 and 0.86. The maximum circularity is maintained for 25 × 10^3 cells; however, high circularity value was obtained for all cell densities showing there is no correlation between cell seeding density and circularity.

3.3. Effect of Paramagnetic Agent on Tunable 3D Cellular Structures. In our previous study[8] varied Gd^{3+} chelates and salts, such as gadobutrol, gadoteric acid, and gadodiamide, were used as a paramagnetic agent, and they were investigated in terms of cellular toxicity. Compared to other paramagnetic agents Gadobutrol (Gx) showed the lowest toxicity on 2D cultured cells; therefore, Gx was used as a paramagnetic agent in this study. The Gx concentration was optimized for the newly developed MagLev setup, which consists of 40 × 5 mm magnets. Various concentrations of Gx (30, 50, and 100 mM) were investigated in terms of levitation capability and cytotoxic effect on NIH/3T3 cells.

Figure 2A represents the live/dead analysis, which also confirms formation of 3D cellular structures via magnetic levitation. High cell viability was observed for the 3D culture of low cell density (2.5 × 10^3) that was cultured during 24 h under varied Gx concentrations (30, 50, 100 mM) as given in Figure 2A and 2B. The diameters of spheroids were below 200 μm. This result supports that diffusion limitation was overcome with the low cell seeding density. Moreover, high Gx concentrations (50 and 100 mM) did not affect the viability of 3D cellular structures contrary to our previous findings where 2D standard cell culture was used.[8] That result emphasizes that different responses are obtained with the same agents when cells are cultured in 2D and 3D, and it confirms that the 3D microenvironment provides better resistance against toxic substances.[46,47] It is worth mentioning that recently the influence of Gx on cell viability was also investigated in 3D spheroids, and it was reported[48,49] that 50 mM Gx provides around 87% viability, which also correlates well with our findings.

Spheroids formed in low cell density were also investigated in terms of spheroid area and circularity as shown in Figure 2C. The spheroid area was calculated by ImageJ for various Gx concentrations. Increased Gx concentrations lead to increased spheroid area 2.6, 3.6, and 6.8 × 10^3 μm^2 for 30, 50, and 100 mM Gx, respectively, as seen in Figure 2C. Higher paramagnetic agent concentrations caused better magnetization; therefore, more cells were gathered and accumulated in the center close to each other, which triggered formation of bigger spheroids. Also, circularity was obtained as 0.714, 0.843, and 0.905 for 30, 50, and 100 mM Gx, respectively, as given in

https://dx.doi.org/10.1021/acsabm.0c01523
ACS Appl. Bio Mater. 2021, 4, 1794−1802

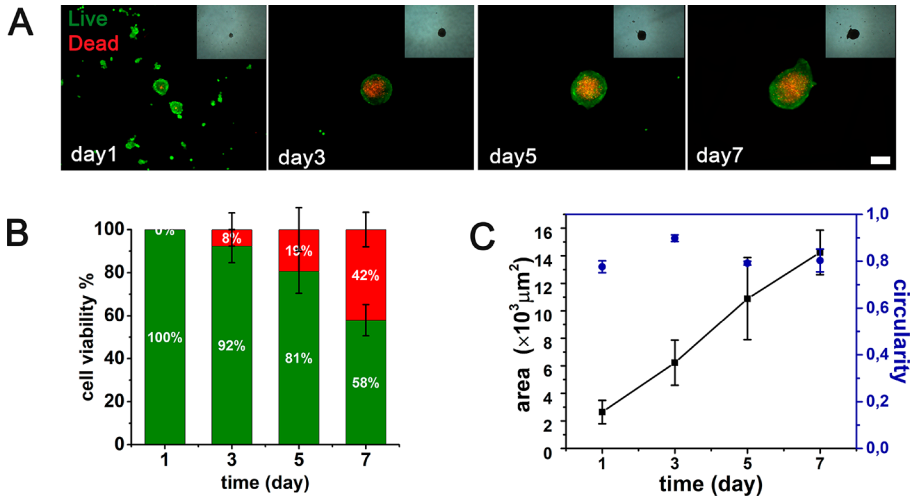

Figure 3. (A) Cell viability images of NIH/3T3 spheroids for various cell culture times (days 1, 3, 5, and 7). Scale bar: 200 μm (green, live cells; red, dead cells). (B) Cell viability values of NIH/3T3 spheroids for various cell culture times (days 1, 3, 5, and 7). (C) Representative spheroid area versus circularity for various cell culture times (days 1, 3, 5, and 7).

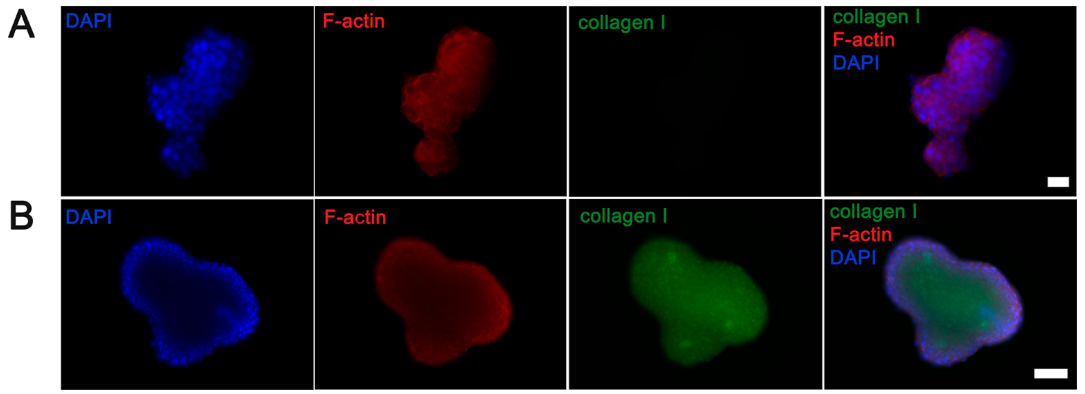

Figure 4. Immunofluorescence staining of NIH/3T3 spheroids for (A) short-term (day 1) (scale bar: 20 μm) and (B) long-term (day 7) cell cultures (scale bar: 50 μm).

Figure 2C. Those results confirm that high Gx concentration not only supports formation of bigger 3D cellular structures but also improves the circularity of the 3D cellular structures. It was shown that both spheroid size and circularity could be tuned by applying different Gx concentrations.

3.4. Effect of Culturing Time on Tunable 3D Cellular Structures. Another parameter that affects the cell viability, spheroid size, structure, and cellular properties is culture time. Here, we investigated the cell viability and morphological changes of spheroids obtained with NIH/3T3 cells for long-term (1/3/5/7 day) culturing. Long-term culturing was done at 30 mM Gx and 2.5 × 10^3 cell numbers while using a 40 × 5 mm magnet (0.15 T). As shown in Figure 3A and Figure 3B, cell viability decreased with increasing culture time, while necrotic core formation was observed starting from day 3. On day 3, the diameter of the spheroid reached 200 μm and that led to diffusion limitation; therefore, cell viability decreased to 92%. Further, on day 5 and day 7, cell viability decreased to 81% and 58%, respectively. As discussed previously, above 200 μm of spheroid diameter diffusion limitation occurs that results in low cell viability. With increasing culturing time, bigger spheroids and larger spheroid area were obtained as given in Figure 3A and Figure 3C. The spheroid areas were calculated by ImageJ as 2.6, 6.2, 10.9, and 14.2 × 10^3 μm^2 for day 1, day 3, day 5, and day 7, respectively. Obtained circularity values (Figure 3C) that range between 0.78 and 0.9 confirmed that spheroid structure was protected for long culturing times.

In general, spheroids between 10 and 100 μm are used in fundamental studies and drug screening,[50] larger spheroids (100−1000 μm) are used in transplant models for *in vivo* research of animal models and replacement of organs,[51−53] and at about 1000 ± 300 μm of spheroid size, they can be used in regenerative medicine applications.[54,55] The size of a spheroid and formation of a necrotic core is also and important property for a tumor model because it needs to mimic the *in vivo* tumor very closely. It is well-known that spheroid models including the necrotic core are more resistant to chemo- and radiotherapies compared to 2D cell cultures.[21,56] Therefore, we foresee that the developed models would be effective alternatives to regular methodologies for the formation of 3D spheroid tumor models with tunable properties.

3.5. Characterization of 3D Cellular Structures. To analyze the cellular morphology within 3D cellular structures and to demonstrate the secretion of cellular and extracellular components, immunofluorescence staining was performed for F-Actin, nuclei, and Collagen Type-I both for short-term (day 1) and long-term (day 7) cultured spheroids. In spheroid formation, it is known that cellular aggregation occurs by spontaneous cell−cell interaction. In addition to this, cells secrete their ECM molecules into the aggregate to form a solid

https://dx.doi.org/10.1021/acsabm.0c01523
ACS Appl. Bio Mater. 2021, 4, 1794−1802

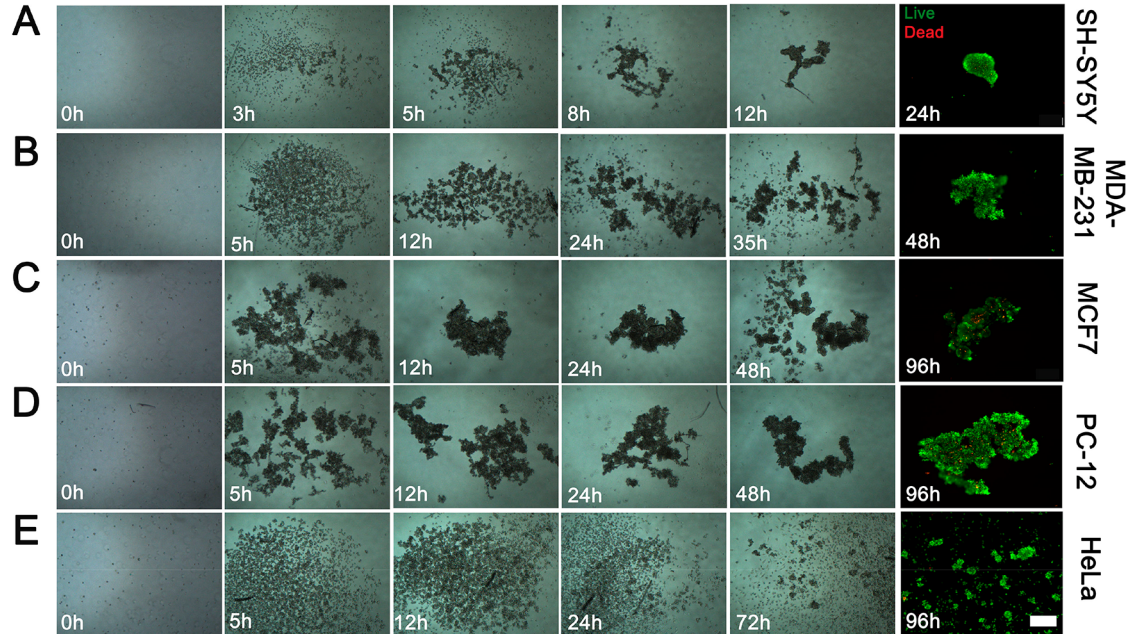

Figure 5. Time-dependent light microscopy images of 3D tumor spheroid formation via magnetic levitational assembly and cell viability of 3D tumor spheroids for different cancer cell lines: (A) SH-SY5Y, (B) MDA-MB-231, (C) MCF7, (D) PC-12, and (E) HeLa. Scale bar: 100 μm

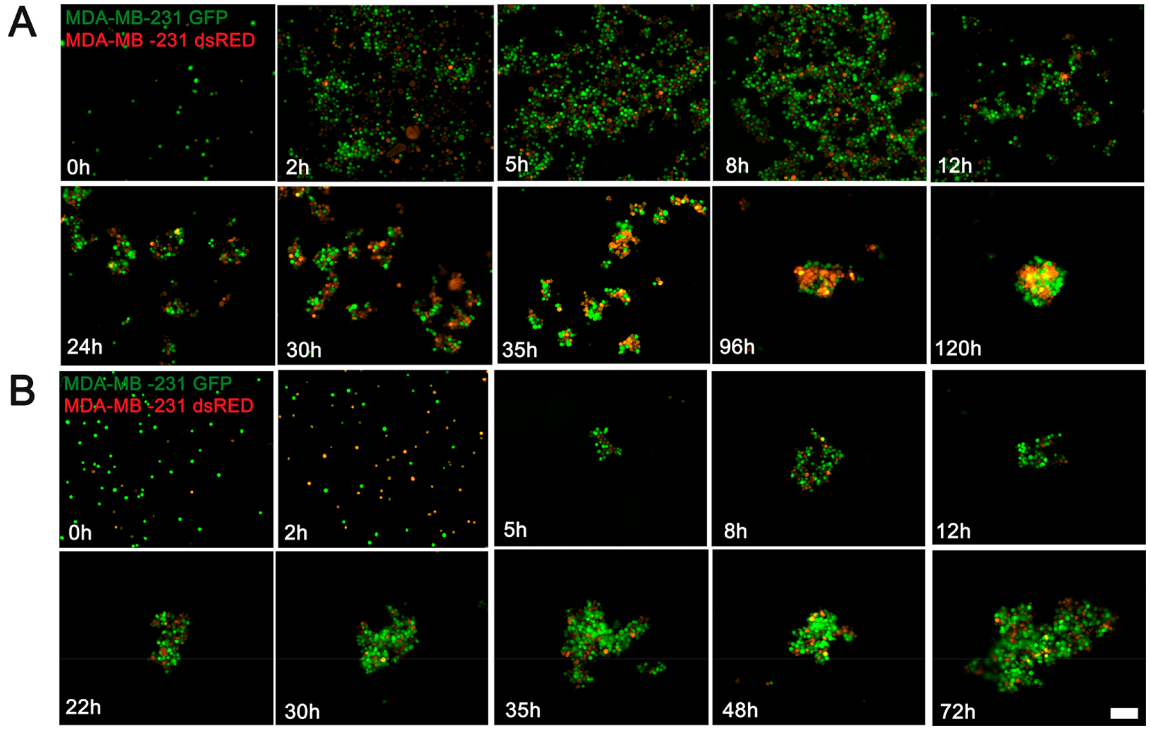

Figure 6. Time-dependent fluorescent microscopy images of 3D coculture model formation for various Gx concentrations: (A) 50 mM Gx and (B) 100 mM Gx. Scale bar: 100 μm.

spheroid structure.[57] As shown in Figure 4A, cells started to interact with each other starting from day 1 and formed 3D cellular structures, where nuclei of cells and actin filaments were observed clearly. During 7-day culturing, cells continued to proliferate and much larger spheroid structures were formed. Collagen is one of the major ECM constituents; therefore, ECM formation was confirmed within the 7-day cultured spheroids by positive staining for Collagen Type-I, while no Collagen secretion was observed for day 1 samples indicating that a 24 h culture time is not enough for ECM formation.

3.6. Formation of 3D Tumor Structures from Different Cell Lines via Magnetic Levitation. The applicability of the system was tested on 3D tumor formation by using different cell lines. At first, the ability to magnetically manipulate cells in 3D was tested with healthy NIH/3T3 fibroblast cells. After optimized parameters were obtained, varied cancer cell lines (MCF7, MDA-MB-231, SH-SY5Y, PC-

https://dx.doi.org/10.1021/acsabm.0c01523
ACS Appl. Bio Mater. 2021, 4, 1794−1802

12, and HeLa) were investigated in terms of 3D spheroid formation. Figure 5 represents the time-dependent 3D spheroid formation and viability analysis of spheroids obtained from varied cell lines. SH-SY5Y cells form smaller and more cohesive spheroids only in 24 h, while other cells form less dense and loose 3D cellular structures for longer culture times. Especially HeLa cells form much smaller and intermittent cell aggregates at 96 h. These differences can be attributed to cell adhesion molecule (CAM) and extracellular matrix (ECM) profiles of each cell type, where SH-SY5Y cells show high-expression levels of CAMs[58] leading to compact spheroid formation and MD-MBA-231 cells have been known for lack of tight cell−cell interaction[59] resulting in formation of loose 3D cellular structures. It was observed that the spheroid morphology is directly related with the type of cell and cell line, but it can also be manipulated by changing system parameters.

Taken together, these results further indicate the applicability of the MagLev system on 3D tumor spheroid formation while highlighting the effect of CAM and ECM molecules to promote cell−cell adhesion and cellular assembly.

3.7. Formation of Tunable 3D Coculture Models via Magnetic Levitation. Coculture models are more realistic and dependable systems to mimic native tissues, and they are commonly utilized for varied tissue engineering studies, such as drug research on 3D tumor models.[60−62] Here, 3D coculture assembly was demonstrated by using MDA-MB-231 GFP and MDA-MB-231 dsRED cells. Gx concentration was changed to tune the size and the formation time of spheroids for the same cell-density. Smaller coculture models were formed in longer incubation time when 50 mM Gx was used (Figure 6A), and coculture assembly started to form at 24 h. The number of smaller cellular aggregates increased in time and merged into bigger aggregates. On the other hand, higher Gx concentration (100 mM) promoted faster and bigger coculture assembly, where cellular aggregates started to form at 5 h (Figure 6B) and continued to proliferate with time to form much larger 3D coculture structures.

4. CONCLUSION

In conclusion, we have demonstrated formation of tunable 3D cellular structures and spheroids via a newly developed MagLev setup. The reported MagLev methodology is simple, rapid, and cost-effective and requires simple components. Also, it offers important advantages such as easy cell medium changing and easy visualization of 3D cellular structures under a light microscope, and also it allows applying postexperimental procedures such as staining and drug screening assays within the same Petri dish. The proposed methodology enables fabrication of tunable spheroids where spheroid size, area, and circularity, and even necrotic core formation, can be controlled by changing cell seeding density, Gx concentration, and culturing time. As a proof-of-concept we have demonstrated the formation of tunable 3D cellular structures by culturing NIH/3T3 cells through magnetic levitational assembly. Furthermore, 3D tumor spheroid formation and coculture models were successfully shown to demonstrate the capability of the MagLev setup. Overall, the obtained results demonstrated the potential of the developed MagLev setup as a tool for 3D cell culture studies. This emerging tool can fulfill the need in various areas; such as drug screening, regenerative medicine, tumor, and disease modeling studies.

ASSOCIATED CONTENT

Supporting Information

The Supporting Information is available free of charge at https://pubs.acs.org/doi/10.1021/acsabm.0c01523.

High volume MagLev setup for 3D cellular structure fabrication: top view, side view, and schematic representation of developed magnetic levitation methodology (PDF)

AUTHOR INFORMATION

Corresponding Author

Ahu Arslan Yildiz − *Department of Bioengineering, Izmir Institute of Technology (IZTECH), 35430 Izmir, Turkey;* orcid.org/0000-0003-0348-0575; Email: ahuarslan@iyte.edu.tr

Author

Rabia Onbas − *Department of Bioengineering, Izmir Institute of Technology (IZTECH), 35430 Izmir, Turkey*

Complete contact information is available at: https://pubs.acs.org/10.1021/acsabm.0c01523

Notes

The authors declare no competing financial interest.

ACKNOWLEDGMENTS

This study was financially supported by TUBITAK (119Z569) and IZTECH-BAP (2020IYTE0006). R.O. gratefully acknowledges the TUBITAK 2211-A National Graduate Scholarship Program. We would like to acknowledge Izmir Institute of Technology, Biotechnology and Bioengineering Research and Application Center (IZTECH-BIOMER) for the microscopy facilities. We also would like to thank Burcu Fıratlıgil for providing MDA-MB-231 dsRED and MDA-MB-231 GFP cell lines.

REFERENCES

(1) Marchioli, G.; van Gurp, L.; van Krieken, P. P.; Stamatialis, D.; Engelse, M.; van Blitterswijk, C. A.; Karperien, M. B.; de Koning, E.; Alblas, J.; Moroni, L.; van Apeldoorn, A. A. Fabrication of three-dimensional bioplotted hydrogel scaffolds for islets of Langerhans transplantation. *Biofabrication* **2015**, *7* (2), 025009.

(2) Salgado, A. J.; Coutinho, O. P.; Reis, R. L. Novel starch-based scaffolds for bone tissue engineering: cytotoxicity, cell culture, and protein expression. *Tissue Eng.* **2004**, *10* (3−4), 465−74.

(3) Marler, J. J.; Upton, J.; Langer, R.; Vacanti, J. P. Transplantation of cells in matrices for tissue regeneration. *Adv. Drug Delivery Rev.* **1998**, *33* (1−2), 165−182.

(4) Forsythe, S. D.; Devarasetty, M.; Shupe, T.; Bishop, C.; Atala, A.; Soker, S.; Skardal, A. Environmental Toxin Screening Using Human-Derived 3D Bioengineered Liver and Cardiac Organoids. *Front Public Health* **2018**, *6*, 103.

(5) Gencoglu, M. F.; Barney, L. E.; Hall, C. L.; Brooks, E. A.; Schwartz, A. D.; Corbett, D. C.; Stevens, K. R.; Peyton, S. R. Comparative Study of Multicellular Tumor Spheroid Formation Methods and Implications for Drug Screening. *ACS Biomater. Sci. Eng.* **2018**, *4* (2), 410−420.

(6) Breslin, S.; O'Driscoll, L. Three-dimensional cell culture: the missing link in drug discovery. *Drug Discovery Today* **2013**, *18* (5−6), 240−9.

(7) Sun, T.; Jackson, S.; Haycock, J. W.; MacNeil, S. Culture of skin cells in 3D rather than 2D improves their ability to survive exposure to cytotoxic agents. *J. Biotechnol.* **2006**, *122* (3), 372−81.

(8) Turker, E.; Demircak, N.; Arslan Yildiz, A., Scaffold-free cell culturing in three-dimension using magnetic levitation. *Biomater. Sci.* **2018**, *6*, 1745.
(9) Mironov, V.; Visconti, R. P.; Kasyanov, V.; Forgacs, G.; Drake, C. J.; Markwald, R. R. Organ printing: tissue spheroids as building blocks. *Biomaterials* **2009**, *30* (12), 2164−74.
(10) Monteiro, M. V.; Gaspar, V. M.; Ferreira, L. P.; Mano, J. F. Hydrogel 3D in vitro tumor models for screening cell aggregation mediated drug response. *Biomater. Sci.* **2020**, *8* (7), 1855−1864.
(11) Roudsari, L. C.; Jeffs, S.; West, J. L. Lung adenocarcinoma cell responses in a 3D in vitro Tumor Angiogenesis Model Correlate with Metastatic Capacity. *ACS Biomater. Sci. Eng.* **2018**, *4* (2), 368−377.
(12) Mauney, J. R.; Nguyen, T.; Gillen, K.; Kirker-Head, C.; Gimble, J. M.; Kaplan, D. L. Engineering adipose-like tissue in vitro and in vivo utilizing human bone marrow and adipose-derived mesenchymal stem cells with silk fibroin 3D scaffolds. *Biomaterials* **2007**, *28* (35), 5280−90.
(13) Tung, Y. C.; Hsiao, A. Y.; Allen, S. G.; Torisawa, Y. S.; Ho, M.; Takayama, S. High-throughput 3D spheroid culture and drug testing using a 384 hanging drop array. *Analyst* **2011**, *136* (3), 473−8.
(14) Onbas, R.; Bilginer, R.; Arslan Yildiz, A. On-Chip Drug Screening Technologies for Nanopharmaceutical and Nanomedicine Applications. In *Nanopharmaceuticals: Principles and Applications Vol. 1*; Yata, V. K., Ranjan, S., Dasgupta, N., Lichtfouse, E., Eds.; Springer International Publishing: Cham, 2021; pp 311−346. DOI: DOI: 10.1007/978-3-030-44925-4_8.
(15) Fong, E. L. S.; Toh, T. B.; Yu, H.; Chow, E. K. 3D Culture as a Clinically Relevant Model for Personalized Medicine. *SLAS Technol.* **2017**, *22* (3), 245−253.
(16) Hagemann, J.; Jacobi, C.; Hahn, M.; Schmid, V.; Welz, C.; Schwenk-Zieger, S.; Stauber, R.; Baumeister, P.; Becker, S. Spheroid-based 3D Cell Cultures Enable Personalized Therapy Testing and Drug Discovery in Head and Neck Cancer. *Anticancer Res.* **2017**, *37* (5), 2201−2210.
(17) Xu, X.; Farach-Carson, M. C.; Jia, X. Three-dimensional in vitro tumor models for cancer research and drug evaluation. *Biotechnol. Adv.* **2014**, *32* (7), 1256−68.
(18) Huang, Y.; Fitzpatrick, V.; Zheng, N.; Cheng, R.; Huang, H.; Ghezzi, C.; Kaplan, D. L.; Yang, C. Self-Folding 3D Silk Biomaterial Rolls to Facilitate Axon and Bone Regeneration. *Adv. Healthc Mater.* **2020**, *9* (18), e2000530.
(19) Reininger-Mack, A.; Thielecke, H.; Robitzki, A. A 3D-biohybrid systems: applications in drug screening. *Trends Biotechnol.* **2002**, *20* (2), 56−61.
(20) Edmondson, R.; Broglie, J. J.; Adcock, A. F.; Yang, L. Three-dimensional cell culture systems and their applications in drug discovery and cell-based biosensors. *Assay Drug Dev. Technol.* **2014**, *12* (4), 207−18.
(21) Mehta, G.; Hsiao, A. Y.; Ingram, M.; Luker, G. D.; Takayama, S. Opportunities and challenges for use of tumor spheroids as models to test drug delivery and efficacy. *J. Controlled Release* **2012**, *164* (2), 192−204.
(22) Leung, B. M.; Lesher-Perez, S. C.; Matsuoka, T.; Moraes, C.; Takayama, S. Media additives to promote spheroid circularity and compactness in hanging drop platform. *Biomater. Sci.* **2015**, *3* (2), 336−44.
(23) Fang, G.; Lu, H.; Law, A.; Gallego-Ortega, D.; Jin, D.; Lin, G. Gradient-sized control of tumor spheroids on a single chip. *Lab Chip* **2019**, *19* (24), 4093−4103.
(24) Costa, E. C.; de Melo-Diogo, D.; Moreira, A. F.; Carvalho, M. P.; Correia, I. J. Spheroids Formation on Non-Adhesive Surfaces by Liquid Overlay Technique: Considerations and Practical Approaches. *Biotechnol. J.* **2018**, *13* (1), 1700417.
(25) Okubo, H.; Matsushita, M.; Kamachi, H.; Kawai, T.; Takahashi, M.; Fujimoto, T.; Nishikawa, K.; Todo, S. A novel method for faster formation of rat liver cell spheroids. *Artif. Organs* **2002**, *26* (6), 497−505.
(26) Timmins, N. E.; Dietmair, S.; Nielsen, L. K. Hanging-drop multicellular spheroids as a model of tumour angiogenesis. *Angiogenesis* **2004**, *7*, 97−103.
(27) Tan, Y.; Suarez, A.; Garza, M.; Khan, A. A.; Elisseeff, J.; Coon, D. Human fibroblast-macrophage tissue spheroids demonstrate ratio-dependent fibrotic activity for in vitro fibrogenesis model development. *Biomater. Sci.* **2020**, *8* (7), 1951−1960.
(28) Lin, R. Z.; Chang, H. Y. Recent advances in three-dimensional multicellular spheroid culture for biomedical research. *Biotechnol. J.* **2008**, *3* (9−10), 1172−84.
(29) Cui, X.; Hartanto, Y.; Zhang, H. Advances in multicellular spheroids formation. *J. R. Soc., Interface* **2017**, *14* (127), 20160877.
(30) Ware, M. J.; Colbert, K.; Keshishian, V.; Ho, J.; Corr, S. J.; Curley, S. A.; Godin, B. Generation of Homogenous Three-Dimensional Pancreatic Cancer Cell Spheroids Using an Improved Hanging Drop Technique. *Tissue Eng., Part C* **2016**, *22* (4), 312−21.
(31) Shi, W.; Kwon, J.; Huang, Y.; Tan, J.; Uhl, C. G.; He, R.; Zhou, C.; Liu, Y. Facile Tumor Spheroids Formation in Large Quantity with Controllable Size and High Uniformity. *Sci. Rep.* **2018**, *8* (1), 6837.
(32) Souza, G. R.; Molina, J. R.; Raphael, R. M.; Ozawa, M. G.; Stark, D. J.; Levin, C. S.; Bronk, L. F.; Ananta, J. S.; Mandelin, J.; Georgescu, M. M.; Bankson, J. A.; Gelovani, J. G.; Killian, T. C.; Arap, W.; Pasqualini, R. Three-dimensional tissue culture based on magnetic cell levitation. *Nat. Nanotechnol.* **2010**, *5* (4), 291−6.
(33) Haisler, W. L.; Timm, D. M.; Gage, J. A.; Tseng, H.; Killian, T. C.; Souza, G. R. Three-dimensional cell culturing by magnetic levitation. *Nat. Protoc.* **2013**, *8* (10), 1940−9.
(34) Daquinag, A. C.; Souza, G. R.; Kolonin, M. G. Adipose tissue engineering in three-dimensional levitation tissue culture system based on magnetic nanoparticles. *Tissue Eng., Part C* **2013**, *19* (5), 336−44.
(35) Turker, E.; Arslan-Yildiz, A. Recent Advances in Magnetic Levitation: A Biological Approach from Diagnostics to Tissue Engineering. *ACS Biomater. Sci. Eng.* **2018**, *4* (3), 787−799.
(36) Tasoglu, S.; Yu, C. H.; Liaudanskaya, V.; Guven, S.; Migliaresi, C.; Demirci, U. Magnetic Levitational Assembly for Living Material Fabrication. *Adv. Healthcare Mater.* **2015**, *4* (10), 1469−76.
(37) Tseng, H.; Gage, J. A.; Raphael, R. M.; Moore, R. H.; Killian, T. C.; Grande-Allen, K. J.; Souza, G. R. Assembly of a three-dimensional multitype bronchiole coculture model using magnetic levitation. *Tissue Eng., Part C* **2013**, *19* (9), 665−75.
(38) Tseng, H.; Balaoing, L. R.; Grigoryan, B.; Raphael, R. M.; Killian, T. C.; Souza, G. R.; Grande-Allen, K. J. A three-dimensional co-culture model of the aortic valve using magnetic levitation. *Acta Biomater.* **2014**, *10* (1), 173−82.
(39) Parfenov, V. A.; Koudan, E. V.; Bulanova, E. A.; Karalkin, P. A.; F, D. A. S. P.; Norkin, N. E.; Knyazeva, A. D.; Gryadunova, A. A.; Petrov, O. F.; Vasiliev, M. M.; Myasnikov, M. I.; Chernikov, V. P.; Kasyanov, V. A.; Marchenkov, A. Y.; Brakke, K.; Khesuani, Y. D.; Demirci, U.; Mironov, V. A. Scaffold-free, label-free and nozzle-free biofabrication technology using magnetic levitational assembly. *Biofabrication* **2018**, *10* (3), 034104.
(40) Parfenov, V. A.; Mironov, V. A.; van Kampen, K. A.; Karalkin, P. A.; Koudan, E. V.; Pereira, F. D.; Petrov, S. V.; Nezhurina, E. K.; Petrov, O. F.; Myasnikov, M.; Walboomers, F. X.; Engelkamp, H.; Christianen, P.; Khesuani, Y. D.; Moroni, L.; Mota, C. Scaffold-free and label-free biofabrication technology using levitational assembly in high magnetic field. *Biofabrication* **2020**, *12*, 045022.
(41) Gupta, T.; Aithal, S.; Mishriki, S.; Sahu, R. P.; Geng, F.; Puri, I. K. Label-Free Magnetic-Field-Assisted Assembly of Layer-on-Layer Cellular Structures. *ACS Biomater. Sci. Eng.* **2020**, *6* (7), 4294−4303.
(42) Mishriki, S.; Aithal, S.; Gupta, T.; Sahu, R. P.; Geng, F.; Puri, I. K. Fibroblasts Accelerate Formation and Improve Reproducibility of 3D Cellular Structures Printed with Magnetic Assistance. *Research* **2020**, *2020*, 1−15.
(43) Hirschhaeuser, F.; Menne, H.; Dittfeld, C.; West, J.; Mueller-Klieser, W.; Kunz-Schughart, L. A. Multicellular tumor spheroids: an underestimated tool is catching up again. *J. Biotechnol.* **2010**, *148* (1), 3−15.

https://dx.doi.org/10.1021/acsabm.0c01523
ACS Appl. Bio Mater. 2021, 4, 1794−1802

(44) Mueller-Klieser, W. Tumor biology and experimental therapeutics. *Critical Reviews in Oncology:Hematology* **2000**, *36*, 123−139.
(45) Nath, S.; Devi, G. R. Three-dimensional culture systems in cancer research: Focus on tumor spheroid model. *Pharmacol. Ther.* **2016**, *163*, 94−108.
(46) Fontoura, J. C.; Viezzer, C.; Dos Santos, F. G.; Ligabue, R. A.; Weinlich, R.; Puga, R. D.; Antonow, D.; Severino, P.; Bonorino, C. Comparison of 2D and 3D cell culture models for cell growth, gene expression and drug resistance. *Mater. Sci. Eng., C* **2020**, *107*, 110264.
(47) Weaver, V. M.; vre, S. L.; Lakins, J. N.; Chrenek, M. A.; Jones, J. C. R.; Giancotti, F.; Werb, Z.; Bissell, M. J. beta_4 integrin-dependent formation of polarized three-dimensional architecture confers resistance to apoptosisin normal and malignant mammary epithelium. *Cancer Cell* **2002**, *2* (3), 205−216.
(48) Parfenov, V. A.; Koudan, E. V.; Krokhmal, A. A.; Annenkova, E. A.; Petrov, S. V.; Pereira, F.; Karalkin, P. A.; Nezhurina, E. K.; Gryadunova, A. A.; Bulanova, E. A.; Sapozhnikov, O. A.; Tsysar, S. A.; Liu, K.; Oosterwijk, E.; van Beuningen, H.; van der Kraan, P.; Granneman, S.; Engelkamp, H.; Christianen, P.; Kasyanov, V.; Khesuani, Y. D.; Mironov, V. A. Biofabrication of a Functional Tubular Construct from Tissue Spheroids Using Magnetoacoustic Levitational Directed Assembly. *Adv. Healthc Mater.* **2020**, e2000721.
(49) Parfenov, V. A.; Khesuani, Y. D.; Petrov, S. V.; Karalkin, P. A.; Koudan, E. V.; Nezhurina, E. K.; Pereira, F. D.; Krokhmal, A. A.; Gryadunova, A. A.; Bulanova, E. A.; Vakhrushev, I. V.; Babichenko, I. I.; Kasyanov, V.; Petrov, O. F.; Vasiliev, M. M.; Brakke, K.; Belousov, S. I.; Grigoriev, T. E.; Ekaterina, E. O. O.; Rossiyskaya, I.; Buravkova, L. B.; Kononenko, O. D.; Demirci, U.; Mironov, V. A. Magnetic levitational bioassembly of 3D tissue construct in space. *Sci. Adv.* **2020**, *6* (29), eaba4174.
(50) Theodoraki, M. A.; Rezende, C. O.; Chantarasriwong, O.; Corben, A. D.; Theodorakis, E. A.; Alpaugh, M. L. Spontaneously-forming spheroids as an in vitro cancer cell model for anticancer drug screening. *Oncotarget* **2015**, *6* (25), 21255−21267.
(51) Kawai, Y.; Tohyama, S.; Shimizu, H.; Fukuda, K.; Kobayashi, E. Pigs as Models of Preclinical Studies and In Vivo Bioreactors for Generation of Human Organs. In *Xenotransplantation - Comprehensive Study*; Miyagawa, S., Ed.; IntechOpen, 2019. DOI: 10.5772/intechopen.90202.
(52) Rezende, R. A.; Pereira, F. D. A. S.; Kasyanov, V.; Kemmoku, D. T.; Maia, I.; da Silva, J. V. L.; Mironov, V. Scalable Biofabrication of Tissue Spheroids for Organ Printing. *Procedia CIRP* **2013**, *5*, 276−281.
(53) Yu, Y.; Ozbolat, I. T. Tissue strands as "bioink" for scale-up organ printing. *Annu. Int. Conf IEEE Eng. Med. Biol. Soc. 2014* **2014**, 1428−31.
(54) Ota, H.; Miki, N. Microtechnology-based three-dimensional spheroid formation. *Front. Biosci., Elite Ed.* **2013**, *5*, 37−48.
(55) Lee, J. I.; Sato, M.; Kim, H. W.; Mochida, J. Transplantatation of scaffold-free spheroids composed of synovium-derived cells and chondrocytes for the treatment of cartilage defects of the knee. *Eur. Cell Mater.* **2011**, *22*, 275−90.
(56) Torisawa, Y.-s.; Takagi, A.; Shiku, H.; Yasukawa, T.; Matsue, T. A multicellular spheroid-based drug sensitivity test by scanning electrochemical microscopy. *Oncol. Rep.* **2005**, *13*, 1107−1112.
(57) Smyrek, I.; Mathew, B.; Fischer, S. C.; Lissek, S. M.; Becker, S.; Stelzer, E. H. K. E-cadherin, actin, microtubules and FAK dominate different spheroid formation phases and important elements of tissue integrity. *Biol. Open* **2019**, *8* (1), bio037051.
(58) Jung, G. S.; Lee, K. M.; Park, J. K.; Choi, S. K.; Jeon, W. B. Morphogenetic and neuronal characterization of human neuroblastoma multicellular spheroids cultured under undifferentiated and all-trans-retinoic acid-differentiated conditions. *BMB Rep* **2013**, *46* (5), 276−81.
(59) Ivascu, A.; Kubbies, M. Diversity of cell-mediated adhesions in breast cancer spheroids. *Int. J. Oncol.* **2007**, *31*, 1403−1413.
(60) Tredan, O.; Galmarini, C. M.; Patel, K.; Tannock, I. F. Drug resistance and the solid tumor microenvironment. *J. Natl. Cancer Inst* **2007**, *99* (19), 1441−54.
(61) Kassim, Y. L.; Tawil, E. A.; Buquet, C.; Cerf, D. L.; PierreVannier, J. Three Dimensional Tumor Engineering by Co-Culture of Breast Tumor and Endothelial Cells Using a Hyaluronic Acid Hydrogel Model. *J. Clin. Exp. Oncol.* **2017**, *06* (05), DOI: 10.4172/2324-9110.1000194.
(62) Suurmond, C. E.; Lasli, S.; van den Dolder, F. W.; Ung, A.; Kim, H. J.; Bandaru, P.; Lee, K.; Cho, H. J.; Ahadian, S.; Ashammakhi, N.; Dokmeci, M. R.; Lee, J.; Khademhosseini, A. In Vitro Human Liver Model of Nonalcoholic Steatohepatitis by Coculturing Hepatocytes, Endothelial Cells, and Kupffer Cells. *Adv. Healthcare Mater.* **2019**, *8* (24), e1901379.

https://dx.doi.org/10.1021/acsabm.0c01523
ACS Appl. Bio Mater. 2021, 4, 1794−1802